Photon Total Cross-sections

R.M. Godbole[a] , A. Grau[b], G. Pancheri[c] and Y.N. Srivastava[d]

a: *Centre for Theoretical Studies, Indian Institute of Science, Bangalore, 560 012, India,*

b: *Departamento de Física Teórica y del Cosmos, University of Granada, 18071 Granada, Spain,*

c: *INFN, Frascati National Laboratories, I00044 Frascati, Italy,*

d: *INFN and Physics Department, University of Perugia, I06123 Perugia, Italy.*

ABSTRACT

We discuss present predictions for the total $\gamma\gamma$ and γp cross-sections, highlighting why predictions differ. We present results from the Eikonal Minijet Model and improved predictions based on soft gluon resummation.

Photon Total Cross-sections[*]

R.M. Godbole [a], A. Grau [b], G. Pancheri [c] and Y.N. Srivastava [d].

[a] Centre for Theoretical Studies, Indian Institute of Science, Bangalore 560012, India

[b] Departamento de Física Teórica y del Cosmos, University of Granada, 18071 Granada, Spain

[c] INFN, Frascati National Laboratories, I00044 Frascati, Italy

[d] INFN and Physics Department, University of Perugia, I06123 Perugia, Italy

We discuss present predictions for the total $\gamma\gamma$ and γp cross-sections, highlighting why predictions differ. We present results from the Eikonal Minijet Model and improved predictions based on soft gluon resummation.

1. Present predictions for $\gamma\gamma \rightarrow$ hadrons

Present predictions of $\gamma\gamma \rightarrow hadrons$ at energies covered by the Linear Collider differ by large factors[1], as we show in Fig.1. At $\sqrt{s} = 500\,GeV$ different models can predict values which differ by a factor 3, and the differences widen as the energy increase. We plan, in the following, to discuss a work program to reach stable predictions, based on a QCD description of the decrease and the rise of total cross-sections through Soft Gluon Summation (Bloch-Nordsieck Model) and Mini-jets. There are different reasons why predictions differ so widely one from the other, some of which are related to the fact that there is no calculation to obtain quantitative descriptions of total cross-sections from first principles. This would not necessarily be a deterrent from making correct predictions, as the $pp/p\bar{p}$ case shows. In Fig. 2 we show present data and some model predictions for the proton case. Another important reason for the variety of predictions is that all models for $\gamma\gamma$ apply some degree of extrapolation from γp and $pp/p\bar{p}$ data. Since, for both photon and proton processes, there are still differences among data at high energy (although within one or two standard deviations at most) this ends up doubling the errors in the extrapolation to $\gamma\gamma$. The present range
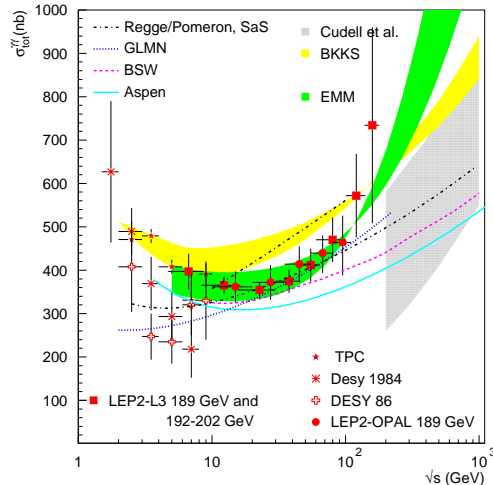

Figure 1. Predictions for $\gamma\gamma \rightarrow hadrons$ from various models, Aspen [2], SaS[3], BSW[4], GLMN [5], BKKS [6], EMM [7,8] and Cudell et al. [9].

of variability of the high energy data for the photoproduction cross-section is highlighted in Fig. 3, where present data are shown together with the predictions from the Eikonal Minijet Model (EMM)[8].

As for $\gamma\gamma$, it should also be pointed out that at low energies old $\gamma\gamma$ data have large errors and even LEP data [17] may have a 10% normalization error. Finally, $\gamma\gamma$ data do not reach a high enough energy to pinpoint how the cross-section
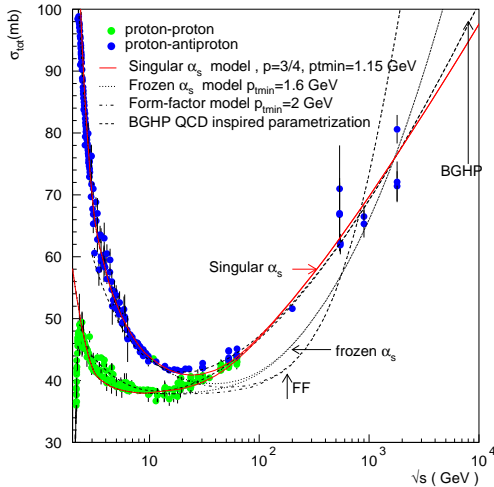
Figure 2. Total proton proton and proton-antiproton cros-section as described by the Aspen model [2](labelled BHGP), and a QCD mini-jet model which includes soft gluon effects[10]. Tevatron data come from E710[11], E811[12] and CDF [13] experiments.

Figure 3. Data for total $\gamma p \to hadrons$ and predictions from the Aspen[2] and EMM[7,8] model. HERA data are from ZEUS [14], H1 [15] and a set of data extrapolated from $Q^2 \neq 0$ from the ZEUS BPC [16].

rises (unlike the $pp/p\bar{p}$ case). These reasons make widely varying predictions for $\gamma\gamma \to hadrons$.

2. Which predictions to trust

We can distinguish between various models by grouping them as those for which the photon is treated like a proton vs. the QCD models. To the first group there belong also models based on Gribov factorization

$$\sigma_{\gamma\gamma} = \frac{\sigma_{\gamma p}^2}{\sigma_{pp/\bar{p}}} \qquad (1)$$

for which $\sigma_{\gamma\gamma}(\sqrt{s} = 1 \ TeV) = 500 \div 700 \ nb$. The QCD based models include the Eikonal Minijet Model (EMM) for which $\sigma_{\gamma\gamma}(\sqrt{s} = 1 \ TeV) = 1000 \div 1500 \ nb$. We show in Fig. 4 two different predictions from the EMM, which will be discussed shortly.

3. QCD vs. stable predictions

A work program to reach stable predictions will be based on treating the photon at low energy like a proton, while distinguishing it from the proton
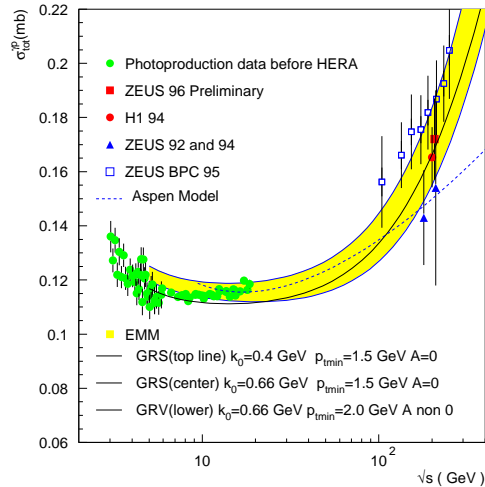
at high energy where QCD processes and parton densities may be different for protons and photons. At the same time it will be important to attempt a unified description for all three processes. The basic expression for the total hadronic cross-section, to be used throughout this paper, will be based on the eikonal approximation, namely

$$\sigma_{tot}^{\gamma h} = 2P_{had}^{\gamma h} \int d^2\vec{b}[1 - e^{-\chi_I(b,s)} \cos\chi_R(b,s)] \quad (2)$$

where $P_{had}^{\gamma h}$ is a phenomenological parameter introduced to describe the probability that a photon behaves like a hadron. Its value can be fixed from Quark Counting rules and Vector Meson Dominance, to be $P_{had}^{\gamma p} = \sum(4\pi\alpha/f_V^2)$, $V = \rho, \omega, \phi$. For $\gamma\gamma$ processes Eq. 2 holds with $P_{had}^{\gamma\gamma} = [P_{had}^{\gamma p}]^2$. Eq. 2 is also used for purely hadronic processes, in which case $P_{had}^{\gamma h} = 1$. We set $\chi_R(b,s) = 0$ and from the expression for the inelastic cross-section, i.e.

$$\sigma_{inel}^{\gamma h} = P_{had}^{\gamma h} \int d^2\vec{b}[1 - e^{-2\chi_I(b,s)}] \qquad (3)$$

we identify $2\chi_I(b,s)$ with the average number $n(b,s)$ of inelastic collisions taking place for any
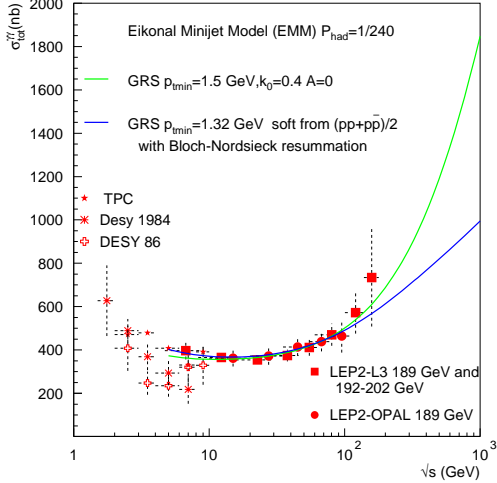
4

Figure 4. Data for $\gamma\gamma \rightarrow hadrons$ and fits using the EMM, with and without soft gluon resumation.

given value of the impact parameter b, at energy $\sqrt{s}$ of the colliding hadrons. In the figures to follow, for all the curves with Bloch-Nordsieck resummation, for γp we have chosen the soft part of $n(b,s)$ as coming only from proton proton, as this seems to give the best description for the soft part, whereas for $\gamma\gamma$ we have chosen the average between pp and $p\bar{p}$. Then, for $\gamma\gamma$

$$n(b,s) = n_{soft}^{\gamma\gamma} + A_{BN}(b,s,p_{tmin})\tilde{\sigma}_{jets}^{\gamma\gamma}(s,p_{tmin}) \quad (4)$$

with $\tilde{\sigma}_{jets}^{\gamma\gamma}(s,p_{tmin}) = \sigma_{jets}^{\gamma\gamma}(s,p_{tmin})/P_{had}^{\gamma\gamma}$. Resummation of soft gluons takes place through the Fourier transform of the exponentiated soft gluon transverse momentum distribution in b space, obtained using the Bloch-Nordsieck (BN) method[10], $e^{-h(b,s,p_{tmin})}$, with

$$h(b,s,p_{tmin}) = \int_{k_{min}}^{k_{max}} d^3 \bar{n}_{gluons}(k) \ [1 - e^{ik_t \cdot b}] \quad (5)$$

In the BN model, the impact parameter space distribution appearing in the eikonal formalism is then identified with

$$A_{BN}(b,s,p_{tmin}) = \frac{e^{-h(b,s,p_{tmin})}}{\int d^2\vec{b} \ e^{-h(b,s,p_{tmin})}} \quad (6)$$

In our work program, we first obtain a good description of proton data[18]. This allows to fix

the soft eikonal to be used together with QCD minijets and resummation for protons. We then try to get a good description of γp using the soft eikonal, and, subsequently, fix the jet parameters, p_{tmin} and densities, to be used with photons.

4. Bloch-Nordsieck resummation

Resummation and its embodyment in the EMM constitute a very challenging task : this involves calculating the function $h(b,s,p_{tmin})$, i.e. fix k_{min} and k_{max} for each parton parton scattering. In our presently simplified approach, we shall average the function $A_{BN}(b,s,p_{tmin})$, and hence k_{max}, over densities and parton cross-sections, obtaining for k_{max} a rising function of the energy $\sqrt{s}$, as discussed in the next section. A second crucial point of the BN approach, comes in setting $k_{min} = 0$. This requires the knowledge of $\alpha_s(k_t)$ as $k_t \rightarrow 0$[19]. We use here the model in [20], with an $\tilde{\alpha}_s$ singular but integrable as discussed in [19], and such that for $k_\perp \gg \Lambda_{QCD}$ $\tilde{\alpha}_s \rightarrow \alpha_s^{AF}$, while for $k_\perp \ll \Lambda_{QCD}$ $\tilde{\alpha}_s \rightarrow (k_\perp^2)^{-p}$. Notice that if p is smaller than 1 the integral in the function $h(b,s,p_{tmin})$ can be done.

5. Energy dependence in impact parameter b

To leading order in α_s the energy dependence which ultimately will soften the rise due to minijets, comes from the maximum transverse momentum allowed to a single gluon emitted by the most energetic partons at the beginning of the QCD cascade, valence quarks for the proton, all type of quarks for the photon. The kinematics for the emission [21] gives

$$k_{max}(\hat{s}) = \frac{\sqrt{\hat{s}}}{2}(1 - \frac{\hat{s}_{jet}}{\hat{s}}) \quad (7)$$

with integration to be done over $\hat{s}$, the energy of the initial parton-parton subprocess and the jet-jet invariant mass $\sqrt{\hat{s}_{jet}}$. Averaging over densities

$$< k_{max}(s) > = \frac{\sqrt{s}}{2} \cdot$$
$$\cdot \frac{\sum_{i,j} \int \frac{dx_1}{\sqrt{x_1}} f_{i/a}(x_1) \int \frac{dx_2}{\sqrt{x_2}} f_{j/b}(x_2) \int dz(1-z)}{\sum_{i,j} \int \frac{dx_1}{x_1} f_{i/a}(x_1) \int \frac{dx_2}{x_2} f_{j/b}(x_2) \int (dz)}$$

with the lower limit of integration in the variable z given by $z_{min} = 4p_{tmin}^2/(sx_1x_2)$.

6. Soft Gluon Emission and Energy Dependence

The Bloch Nordsieck model is like the EMM model with σ_{jet}^{QCD} driving the rise. The Fourier transform of soft gluon emission in k_t space gives the impact parameter space distribution of colliding partons. This introduces an energy dependence in the b-distribution of partons in the hadrons which depends on p_{tmin} and the parton densities. One achieves two main results, a softening effect, and a reduction of the dependence from hard scattering parameters. The softening effect happens because as $\sqrt{s}$ increases, the phase space available for soft gluon emission also increases, and with it the transverse momentum of the initial colliding pair due to soft gluon emission. This leads to more straggling of initial partons and hence to a reduced probability for the collision.

7. Bloch-Nordsieck Model for $p-p$ and $p-\bar{p}$

In the proton-proton and proton-antiproton fit with the Bloch-Nordsieck (BN) model, for the average number of collisions, we now write

$$n(b,s) = \sigma_{soft}A_{BN}^{soft} + \sigma_{jet}A_{BN}^{jet} \qquad (8)$$

where $A_{BN}^{soft}(b,s)$ is obtained using the BN ansätz, with a k_{max} which becomes constant after a slight initial rise. Soft gluon emission has now a twofold effect as the energy increases: with σ_{soft} constant or decreasing (as from Regge exchange) $\sigma_{soft}A_{BN}^{soft}$ will decrease, whereas, with σ_{jet} increasing rapidly, $\sigma_{jet}A_{BN}^{jet}$ will still increase but not as much as without soft gluons. A good description is obtained with a soft part given by

$$\sigma_{soft}^{pp} = \sigma_0 = 48mb \qquad (9)$$

and

$$\sigma_{soft}^{p\bar{p}} = \sigma_0(1 + \frac{2}{\sqrt{s}}) \qquad (10)$$

We show our present description [18] of pp and $p\bar{p}$ data in Fig. 5.

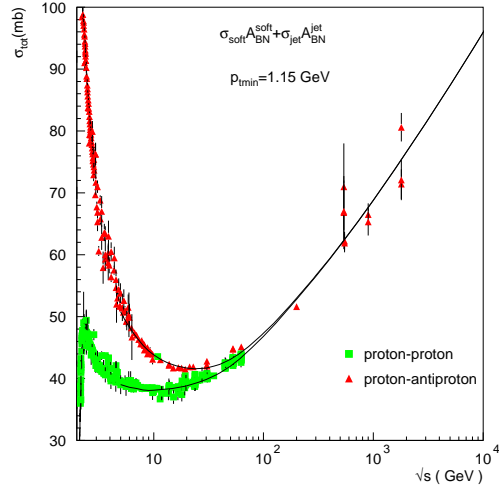

Figure 5. Total proton-proton and proton-antiproton cross-section as described by the EMM with soft gluon emission both in the hard and soft region.

8. The case for γp and $\gamma\gamma$

With the previously described expressions, we now turn to γp, using $n_{soft}^{\gamma p}(b,s) = \frac{2}{3}n_{soft}^{pp}$. We obtain various fits, depending upon the densities being used for the photon, and the results are shown in Figs. 6,7,8, for each set of densities and various values of p_{tmin}. The present update for $\gamma\gamma$ is done using the soft part of the eikonal $n(b,s)$ from the average of the proton and the antiproton fit, i.e. $n_{soft}^{\gamma\gamma}(b,s) = \frac{4}{9}(n_{soft}^{pp} + n_{soft}^{p\bar{p}})/2$, soft resummation for hard scattering, and three types of densities, GRV[22], GRS[23] and CJKL [24]. In Fig. 9, we show a comparison between the predictions from the Aspen model, the EMM without soft gluon emission, and two curves from the EMM with inclusion of soft gluons and different parton densities. We also indicate (stars) pseudo data points to be measured at the future Linear Collider. How predictions for $\gamma\gamma \to hadrons$ depend upon p_{tmin} in the case of CJKL densities, can be seen in Fig. 10. Similar results hold for other densities.

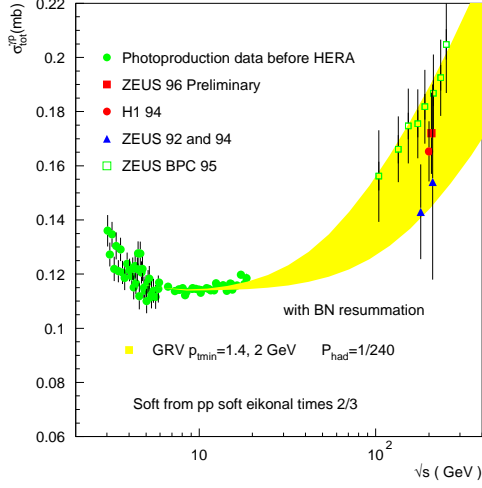Figure 6. Total γp cross-section, with soft gluon resummation (BN) and GRV densities in the mini-jet cross-section.
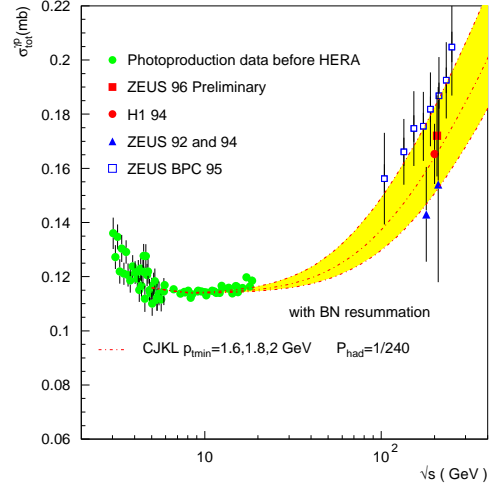

Figure 8. As in Figs.6, 7 with CJKL densities and a set of p_{tmin} values which fit the high energy data.
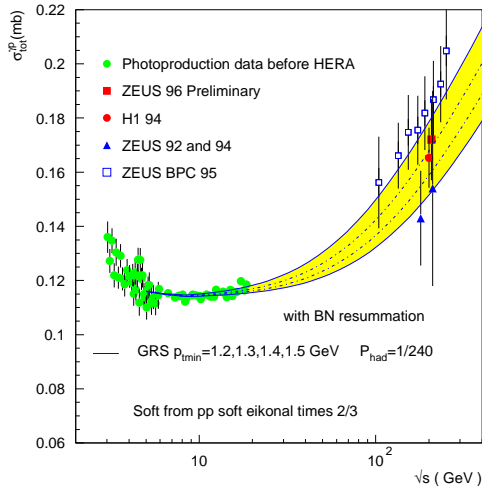

Figure 7. Total γp cross-section, with soft gluon resummation (BN) and GRS densities in the mini-jet cross-section, for an indicative set of values for p_{tmin}.
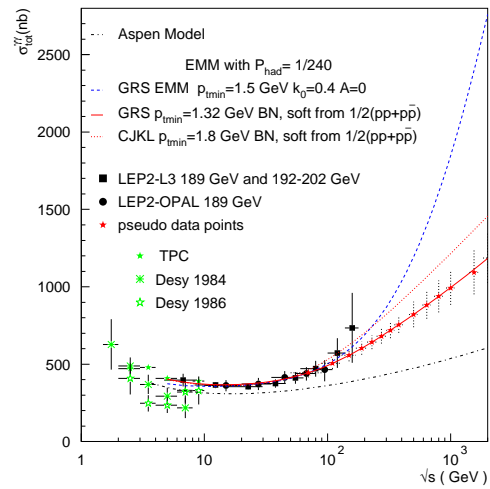

Figure 9. Comparison between the Aspen model and the EMM with and without soft gluons, with pseudo data points to be possibly measured at the Linear Collider.
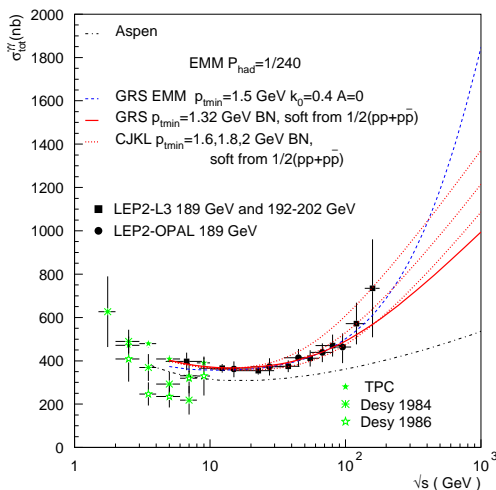
Figure 10. Comparison between the Aspen model and the EMM with and without soft gluons, for different choices of parameters for the mini-jet cross-section.

9. Conclusions

In this talk we have presented a comprehensive description of proton and photon total cross-sections, based on the use of the Eikonal representation and on the hypothesis that QCD jet cross-sections drive the rise of all total cross-sections. This Eikonal Minijet Model (EMM) is not fully satisfactory, since the rise with energy thus predicted is either too fast or too slow, depending on the parameters. It is shown that inclusion of soft gluon emission from initial state partons can give a much more realistic description in all cases, $pp, p\bar{p}, \gamma p$ and $\gamma\gamma$. Different models are also discussed and compared with the data and with the EMM.

Acknowledgements

REFERENCES

1. R.M. Godbole, A. De Roeck, A. Grau and G. Pancheri, JHEP **0306** (2003) 061.
2. M.M. Block, E.M. Gregores, F. Halzen and G. Pancheri, Phys. Rev. **D60** (1999) 054024.
3. G. Schuler and T. Sjöstrand, Z. Phys. **C 68** (1995) 607, Phys. Lett. **B 376** (1996) 193, Z. Phys. **C 73** (1997) 677.
4. C. Bourrelly, J. Soffer and T.T. Wu, Mod. Phys. Lett. **A 15** (2000) 9.
5. E. Gotsman, E. Levin, U. Maor and E. Naftali, Eur. Phys. J. **C 14** (2000) 511.
6. B. Badelek, M. Krawczyk, J. Kwiecinsky and A.M. Stasto, Phys. Rev. **D 62** (2000) 074021.
7. A. Corsetti, R.M. Godbole and G. Pancheri, Phys. Lett. **B 435** (1998) 441.
8. R.M. Godbole and G. Pancheri, Eur. Phys. J.**C 19**:129-136, 2001.
9. J.R. Cudell et al., hep-ph/0212101.
10. A. Grau, G. Pancheri and Y.N. Srivastava, Phys. Rev. **D60** (1999) 114020.
11. E710 collaboration, N.A. Amos et al., Phys. Rev. Lett. **63** (1989) 2784.
12. E811 collaboration, C. Avila et al., Phys. Lett. **B 445** (1999) 419.
13. CDF collaboration, F. Abe et al., Phys. Rev. **D 50** (1994) 5550.
14. ZEUS Collaboration, S. Chekanov et al., Nucl. Phys. **B 627** (2002) 3.
15. H1 collaboration, S. Aid et al., Z. Phys. **C 69** (1995) 27.
16. ZEUS collaboration, J. Breitweg et al., DESY-00-071, hep-ex/0005018.
17. M.M. Block, these Proceedings
18. A. Grau, G. Pancheri and Y.N. Srivastava, *Soft Gluon Resummation and the energy dependence of total cross sections*, in preparation.
19. A. Grau, S. Pacetti, G. Pancheri, Y.N. Srivastava and A. Widom, these Proceedings.
20. A. Nakamura, G. Pancheri and Y.N. Srivastava, Z. Phys. **C21**:243, 1984.
21. P. Chiappetta and M. Greco, Nucl. Phys. **B 199** (1982) 77.
22. M. Glück, E. Reya and A. Vogt, Phys. Rev. **D 46** (1992) 1973.
23. M. Glück, E. Reya and I. Schienbein, Phys. Rev. **D 60** (1999) 054019; Erratum, ibid **D 62** (2000) 019902.
24. F. Cornet, P. Jankowski, M. Krawczyk and A. Lorca, Phys. Rev. **D 68** (2003) 014010.